# HARDWARE IMPLEMENTATION OF A PROPOSED QR-TLS DOA ESTIMATION METHOD AND MUSIC, ESPRIT ALGORITHMS ON NI-PXI PLATFORM

## Nizar Tayem[*], Muhammad Omer, Mohamed El-Lakkis, Syed A. Raza, and Jamal F. Nayfeh

Department of Electrical Engineering, College of Engineering Prince, Mohammad Bin Fahd University, Al-Khobar, Saudi Arabia

**Abstract**—In this paper, we present an experimental verification of a novel QR-TLS algorithm. Two other algorithms for direction of arrival (DOA) estimation of multiple incident source signals called multiple signal classification (MUSIC) and estimation of signal parameters via rotational invariance techniques (ESPRIT) are implemented on a National Instruments (NI) PXI platform. The proposed method is based on subspace decomposition of a received data into a signal and a noise space using QR decomposition. The angle of the signal arrival information is extracted from the signal subspace by using the method of total least squares (TLS). The algorithms are implemented in LabView NI hardware. The experimental procedures are discussed in details which includes interfacing of the uniform linear array (ULA) of antennas with the NI-PXI platform, calibrating phase differences between the RF receivers, and selecting transmitter and receiver parameters, for determining the DOAs of the multiple incident source signals. The experimental results are shown for a single and two sources lying at arbitrary angles from the array reference to verify the successful real time implementation of the proposed and other DOA estimation algorithms.

## 1. INTRODUCTION

Estimating the bearing angles of the multiple incident source signals is an active research area due to its innumerable applications in radar, sonar for source localization, and beam forming/steering in mobile communication. The existing literature in this area focuses mainly

on enhancing the precision, and devising low complexity methods for DOA estimation. The performance of these methods is mostly assessed through numerical simulations [1–5]. However, only few studies extend computer simulations to a realistic implementation for real-time use in practical scenarios. In this regard, a smart antenna system implementation for DOA estimation has appeared in [6–10]. The authors in [6, 7] present an FPGA implementation of a DOA estimation algorithm with emulated sources. Wang and Glesner in [8] employs data acquisition hardware to obtain experimental data in an anechoic chamber. The acquired data is processed off-line for DOA estimation and beam-forming on FPGA. A DSP-based real-time DOA estimator is presented in [11] for determining underwater acoustic source directions in real time.

In this work, we present a hardware implementation of a novel DOA estimation method QR-TLS that we have recently proposed in [12] along with two other well known methods called MUSIC and ESPRIT on NI PXI platform. The proposed QR-TLS method is a subspace decomposition based algorithm for joint frequency of arrival (FOA) and DOA estimation. The method employs QR factorization technique on a Toeplitz structured received data matrix to estimate the signal and noise subspaces. Further more, the proposed method avoids the computations of determining the cross-correlation matrix and applying computationally complex eigen value decomposition (EVD) or singular value decomposition (SVD) for signal subspace as required by the conventional algorithms. QR-TLS Method has less computational load and cost efficient procedure compared to SVD Method which is employed by ESPRIT and MUSIC algorithms. Calculating the least square via SVD for (mxn) matrix requires a computational complexity in order of $O(2mn^2 + 11n^3)$ while least square via QR decomposition using householder transformation in order of $O(mn^2 - n^3/3)$ [13].

The NI PXI is a PC-based platform. It combines PCI electrical-bus features with the modular packaging, specialized synchronized buses and key software features. It is used for high-performance and low-cost deployment of applications such as manufacturing, military and aerospace, machine monitoring and automotive. The NI hardware employed for the DOA estimator is composed of a chassis which includes a stand alone controller and modules with signal transmission/reception capabilities such as RF signal generator, RF down converter, digitizer and RF amplifier. A uniform linear array (ULA) of four omnidirectional antennas is interfaced with the NI-PXI platform. The four receivers are not phase coherent which is caused either by the independent clocks of the receiver modules or

the difference in receiver wire lengths. Thus, a phase calibration step is performed prior to the DOA estimation. The DOA estimator uses MUSIC and ESPRIT methods to achieve accurate DOA of the incident source signal [14]. The DOA estimator is tested in an open atmosphere. The experiment setup and measurement results show that the DOA of incoming sources can be successfully estimated.

The paper is organized as follows. Section 2 discusses the system model and Section 3 highlights the MUSIC and ESPRIT algorithms. In Section 4 the proposed QR-TLS method for DOA estimation is presented. The experimental setup and procedures are discussed in details in Section 5 followed by the experimental results in Section 6. We conclude the paper in Section 7.

## 2. SYSTEM MODEL

The system model assumes $K$ narrowband sources lying in a far-field region of a uniform linear array (ULA) composed of $N$ elements. The model of the signal impinging on the ULA is given as

$$x\left(t\right) = \sum\nolimits_{i=1}^{K} a(\theta_i) s_i\left(t\right) + n(t) \tag{1}$$

which in vector matrix notation can be re-written as

$$x\left(t\right) = A(\theta) s\left(t\right) + n(t) \tag{2}$$

where $x(t)$ is the $(N \times 1)$ received signal vector, $s(t)$ the source signal of dimension of $(K \times 1)$, $n(t)$ the noise vector of dimension $(N \times 1)$, $\theta$ the angle of arrival of multiple sources, and $A$ the $(N \times K)$ dimension array factor matrix and a known matrix that depends on the array geometry.

$$A(\theta) = [a\left(\theta_1\right), a\left(\theta_2\right), \dots, a\left(\theta_K\right)] \tag{3}$$

## 3. MUSIC AND ESPRIT ALGORITHMS

The MUSIC algorithm requires determining of the correlation matrix of the received signal

$$R_x = E\left\{x(t) x^H(t)\right\} \tag{4}$$

where $E[\cdot]$ denotes the mathematical expectation operator, and $H$ is the conjugate transpose.

The eigenvalue decomposition of the matrix $R$ can be expressed as

$$R = U_s D_s U_s^H + U_n D_n U_n^H \tag{5}$$

where $U_s$ spans the signal subspace, and $U_n$ spans the noise subspace. $D_s$ and $D_n$ are the diagonal matrices whose diagonal entries correspond to the eigenvalues associated with $U_s$ and $U_n$ respectively.

The spatial spectrum of the ULA is expressed as

$$S\left(\theta\right) = \frac{1}{a(\theta)^H U_n U_n^H a\left(\theta\right)} \tag{6}$$

The DOA estimates are obtained by scanning the angle $\theta$ in the range $[0°, 180°]$ and observing peaks of the spatial spectrum function $S(\theta)$.

The ESPRIT algorithm divides the ULA into two identical subarrays $X$ and $Y$, displaced from each other by distance $d$.

$$x\left(t\right) = \sum_{i=1}^{K} a(\theta_i)s_i\left(t\right) + n_x(t) \tag{7}$$

$$y\left(t\right) = \sum_{i=1}^{K} a(\theta_i)e^{j\gamma_i}s_i\left(t\right) + n_y(t) \tag{8}$$

where $\gamma_i = \frac{\omega_o d \sin\theta_i}{c}$ is the additional phase shift which the signal goes through at $Y$ as compared to $X$.

In vector matrix notation (7) and (8) can be re-written as

$$x\left(t\right) = A(\theta)s\left(t\right) + n_x(t) \tag{9}$$

$$y\left(t\right) = A(\theta)\varphi s\left(t\right) + n_y(t) \tag{10}$$

where $\varphi$ represents the phase shift between the subarrays given as

$$\varphi = \text{diag}\left(e^{j\gamma_1}, e^{j\gamma_2}, \ldots, e^{j\gamma_k}\right) \tag{11}$$

The objective is to estimate the matrix $\varphi$. For this purpose a new matrix $z(t)$ is defined as

$$z(t) = \begin{bmatrix} x(t) \\ y(t) \end{bmatrix} = \begin{bmatrix} A \\ A\varphi \end{bmatrix} s\left(t\right) + \begin{bmatrix} n_x(\text{t}) \\ n_y(\text{t}) \end{bmatrix} = \bar{A}s\left(t\right) + n_z(t) \tag{12}$$

A correlation matrix of dimension $(2N \times 2N)$ is computed as follows

$$R_z = E\left\{z(t)z^H(t)\right\} \tag{13}$$

Since there are $K$ sources, the $K$ eigenvectors correspond to the $K$ largest eigenvalues form the signal subspace $U_s$. The remaining $2N-K$ eigenvectors represent the noise subspace $U_n$. The space spanned by $U_s$ is the same as that of $\bar{A}$. Therefore, there exists a unique nonsingular $(K \times K)$ matrix $T$ such that

$$U_s = \bar{A}T \tag{14}$$

The matrix $U_s$ is partitioned into two $(N \times K)$ submatrices

$$U_s = \begin{bmatrix} U_x \\ U_y \end{bmatrix} = \begin{bmatrix} AT \\ A\varphi T \end{bmatrix} \tag{15}$$

The columns of both $U_x$ and $U_y$ are linear combinations of $A$, so each of them has a column rank $K$. A new matrix of $U_{xy}$ is defined which has rank $K$

$$U_{xy} = [U_x \quad U_y] \tag{16}$$

Therefore, $U_{xy}$ has a null space of dimension $K$ and there exists a $(2K \times K)$ matrix $F$ such that

$$U_{xy}F = 0 \tag{17}$$

$$[U_x \quad U_y] \begin{bmatrix} F_x \\ F_y \end{bmatrix} = U_x F_x + U_y F_y = 0 \tag{18}$$

$$ATF_x + A\varphi TF_y = 0 \tag{19}$$

Thus, a matrix $\varphi$ is computed from the following expression

$$\varphi = -TF_x F_y^{-1} T^{-1} \tag{20}$$

## 4. PROPOSED QR-TLS METHOD

The ESPRIT algorithm employs computationally complex SVD operation to decompose the received data matrix into signal and noise space. In the proposed method, we replace the SVD operation with a QR factorization which yields the signal and noise space of the data matrix with significantly less computations. Further more, the least square (LS) approach of finding the direction matrix $\varphi$ is replaced with a total least square (TLS) method which is advantageous under noisy measurements of practical scenarios. The following steps are taken in order to estimate the multiple incident source angles.

1) Apply $QR$ decomposition on the observation matrix $z$ to obtain a $2N \times 2N$ matrix $Q$ and $2N \times 1$ matrix $R$.

$$[Q, R] = qr(z) \tag{21}$$

2) From $Q$ the signal space $Q_S$ is obtained by selecting the first $K$ columns.

$$Q_S = [q(1), q(2), \ldots, q(K)] \tag{22}$$

where $q(i)$ denotes the $i$th column of $Q$.

3) The $2N \times K$ matrix $Q_S$ is partitioned into two submatrices $Q_{s1}$ and $Q_{s2}$ where each sub-matrix is of $N \times K$ dimension.

$$Q_S = \begin{bmatrix} Q_{s1} \\ Q_{s2} \end{bmatrix} \tag{23}$$

4) Apply the QR decomposition on the matrix formed as

$$[U, V] = qr\left(Q_s^H Q_s\right) = qr\left(\begin{bmatrix} Q_{s1}^H \\ Q_{s2}^H \end{bmatrix} [Q_{s1} \ Q_{s2}]\right) \tag{24}$$

where $U$, $V$ corresponds to $Q$ and $R$ of the QR factorized results respectively.

5) Partition $U$ into $K \times K$ sub-matrices such that

$$U = \begin{bmatrix} U_{11} & U_{12} \\ U_{21} & U_{22} \end{bmatrix} \tag{25}$$

6) Compute the eigenvalues ($\lambda$'s) of the matrix $H$ given as

$$H = -U_{12}U_{22}^{-1} \tag{26}$$

7) Estimate the elevation angle from the eigenvalues obtained in 4 using the following expression

$$\hat{\theta}_k = \sin^{-1}\left(\frac{\text{angle}(\lambda_k)}{\omega_o d}\right) \tag{27}$$

where $\hat{\theta}_k$ is the estimated DOA of the $k$th source for $k = 1, 2, \ldots, K$.

## 5. EXPERIMENTAL SETUP

An experimental setup is constructed on a flat roof top of a building which emulates as an open atmosphere because of minimal reflecting surfaces. The hardware implementation of the MUSIC and ESPRIT algorithms on the NI PXI platform is performed in two steps. The first step involves physical connections between the NI PXI modules with the transmitter/receiver antennas while in the next step a phase calibration is performed at the receiver end. These steps are explained in the following subsections.

### 5.1. Description of the PXI Chassis

The hardware that we have utilized for implementation and validation purposes employ separate transmission and receiving PXI units. We begin with the brief description of both units in the following.

#### 5.1.1. Transmitter

The NI PXI chassis used for signal transmission is shown in Figure 1. The transmitter unit is equipped with an arbitrary waveform generator
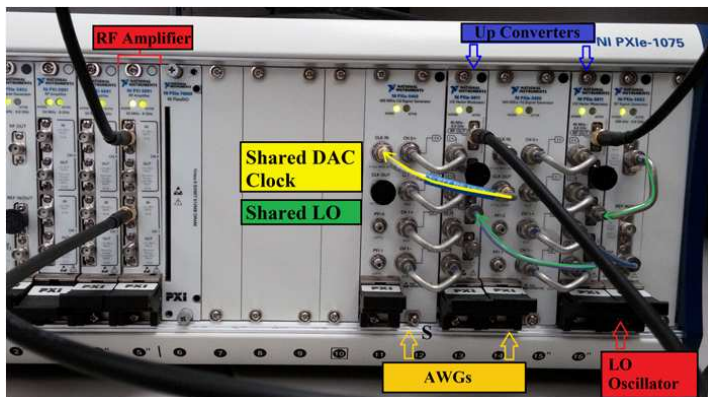
**Figure 1.** NI-PXI transmitter unit.
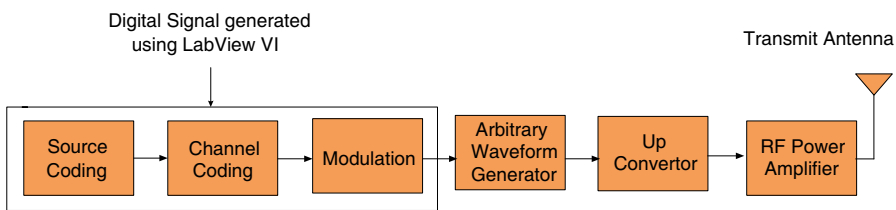


**Figure 2.** Block diagram of the NI-PXI transmitter unit.

(AWG) (NI PXI-5421), upconverter module (NI PXIe-5652), and an RF Amplifier (NI PXI-5691) as shown in Figure 1. The AWG runs at a maximum sampling rate of 100 Mega Samples/s. It is used in conjunction with the upconverter, which takes the input waveform from the LabView and creates a continuous waveform at an intermediate frequency (IF) of 25 MHz and later sends to the upconverter. The upconverter then creates and transmits the desired RF signal. The maximum frequency which the upconverter can transmit is 2.7 GHz. The RF amplifier enhances the signal amplitude which helps in improving the signal to noise ratio.

The block diagram of the NI PXI transmitter unit is shown in Figure 2. In the first stage, a digital signal is generated using LabView functions which involves source coding, channel coding and modulation. Generated signal is then transformed into an analog signal by AWG and is passed to an upconverter module to be converted from an intermediate frequency (IF) signal to a radio frequency (RF) signal. The RF signal is then amplified in the later stage prior to the signal transmission via antenna.

## 5.1.2. Receiver

The receiver is composed of two units. The first unit is an RF downconverter (PXIe-5601) while the second is the high speed digitizer (PXIe-5622). The maximum operating frequency of the downconverter is 2.7 GHz and the bandwidth of 15 MHz. The received signal is downconverted to an IF of 15 MHz which is then forwarded to the digitizer. The digitizer operates at a maximum sampling frequency of 64 Mega Samples/s and is equipped with a digital downconverter chip (DDC) which performs digitization of the IF signal. Figure 3 shows a NI PXI receiver chassis equipped with four receiver units. All these units share same clock which is generated by a local oscillator (LO).

Figure 4 shows the block diagram of the NI PXI receiver unit. The source signal is received through four RF channels and the signal received through each channel is downconverted from RF signal to an IF signal. The IF signals are then converted to digitized discrete signal by ADCs. The outputs of the ADCs are modulated signals in $(I, Q)$ form, from which the amplitude and phase information of the message signal is extracted. In the subsequent stage, three DOA estimation algorithms including MUSIC, ESPRIT and the proposed QR-TLS methods are applied to estimate the unknown source angles $(\theta_1, \theta_2, \ldots, \theta_K)$.



**Figure 3.** NI-PXI receiver unit.
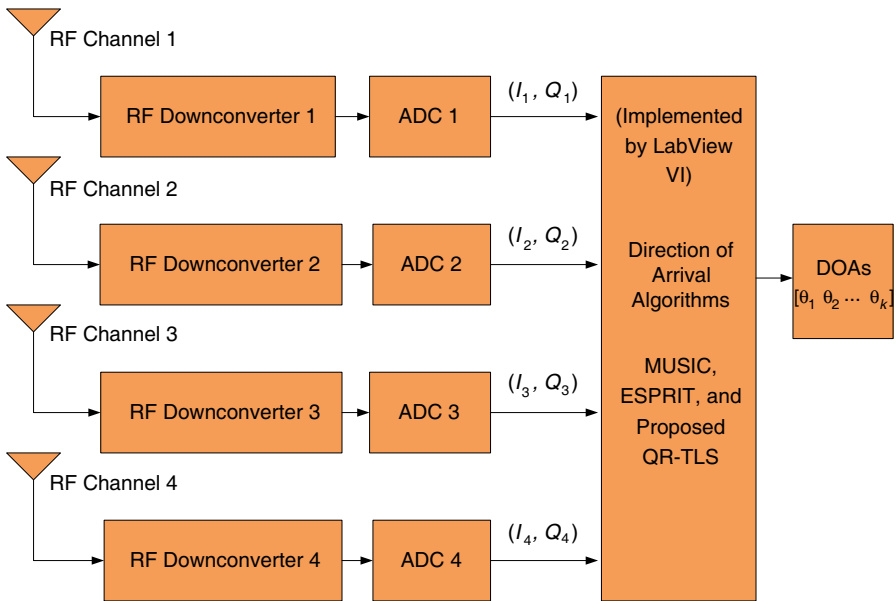
**Figure 4.** Block diagram of the NI-PXI receiver unit.

## 5.2. Setting Up an RF Transmitter and Receivers

An RF transmitter set up is shown in Figure 5 which acts as a source lying in a far field region of a receiver. The NI PXI platform at
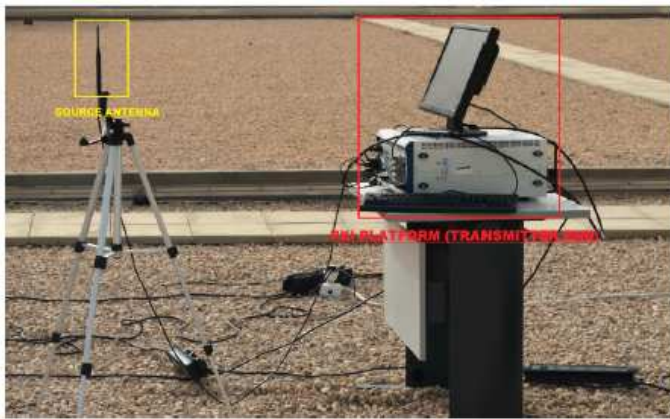


**Figure 5.** PXI platform configured as an RF source.

the transmitter end is equipped with an RF Signal Generator and Upconverter module (NI PXIe-5652), and an RF Amplifier (NI PXIe-5691). The output of the RF amplifier is fed to the antenna mounted on top of a tripod stand.

At the receiver end, a ULA of four omnidirectional wire antennas is configured as shown in Figure 6. The antennas are connected to
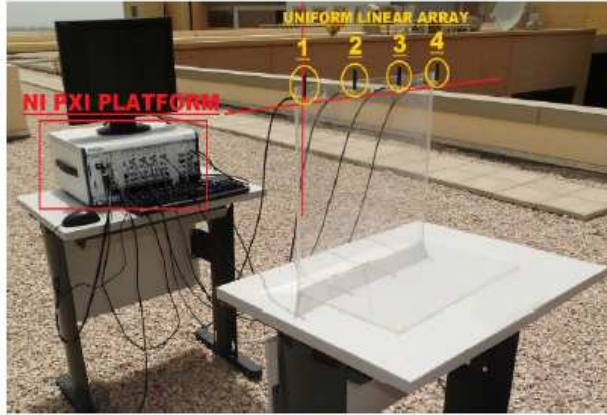


**Figure 6.** ULA of four wire antennas for DOA estimation.

**Table 1.** Experimental parameters for transmitter unit.

| | |
|---|---|
| Total number of antenna elements | 4 |
| Array Geometry | Uniform Linear Array |
| Number of sources | 1, 2 |
| SNR with amplifier | 28 dBm |
| Inter element spacing | $\lambda/2 = 16$ cm |
| Number of snapshots | 10000 |
| Sample per symbol | 8 |
| Symbol rate | 100 k |
| PN sequence order | 9 |
| Modulation Scheme | QPSK |
| Transmit Filter Type | Root raise cosine |
| Filter Length | 8 |
| Alpha | 0.5 |
| Distance between source antenna and ULA | 4.5 m |

RF Downconverter module (NI PXIe-5601). The RF receivers used in the system are independent, which means that each RF receiver has its own local oscillator (LO). The LOs are connected to the same clock signal generated by an RF Signal Generator module (NI PXIe-5652). Table 1 lists the various experimental parameters selected for the implementation purpose.

## 5.3. Phase Calibration at the Receiver End

The initial phase of each LO can be different even when connected to the same clock source. Therefore, a mechanism to calibrate the phase differences of all RF receiver channels is necessary. A four-port RF power divider duplicates the deterministic signal generated by an RF signal generator module into four cophase calibration signals as shown in Figure 7. These calibration signals are then fed to the receiver modules of the NI-PXI and are analyzed for any phase differences via a LabView routine.



**Figure 7.** Setup for calibrating the phase of the received signals.

At this point, the phase difference between the received signals is either caused by the initial phase differences of the LOs or the difference in wire lengths. The front panel of the phase calibration program developed in LabView for phase calibration is shown in Figure 8. The figure shows the initial phase differences between the signal received from the reference antenna and the other three antennas. Once the phase differences are measured, phase offsets are introduced in the received signals to compensate for these phase differences. Figure 9 shows the calibrated signals after introducing phase offset.
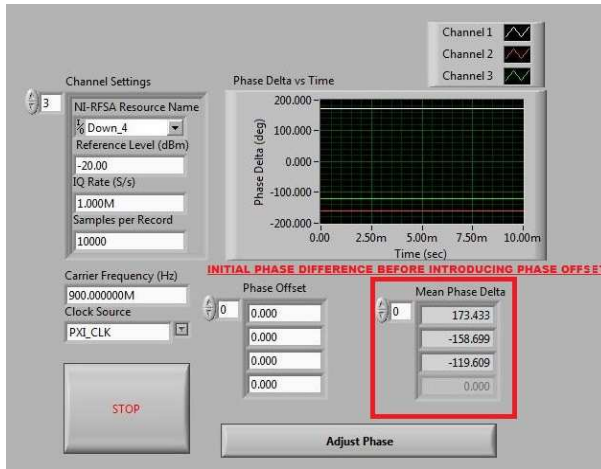
**Figure 8.** Initial phase differences between the received signals.
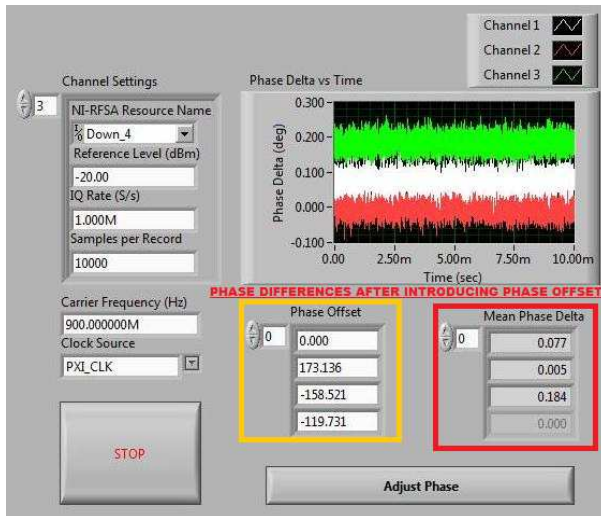


**Figure 9.** Calibrated signals after introducing the phase offset.

## 6. EXPERIMENTAL RESULTS

The performance of the DOA estimator is verified by conducting experiments for a couple of test cases in an open atmosphere for both single and multiple sources placed at arbitrarily selected angles from the array reference.

## 6.1. DOA Estimation for One Source

A single RF source is placed in the far-field region of a ULA at an angle of 100° from the array reference. The first antenna of the ULA is considered as an array reference. The experimental configuration for the first case is shown in Figure 10.
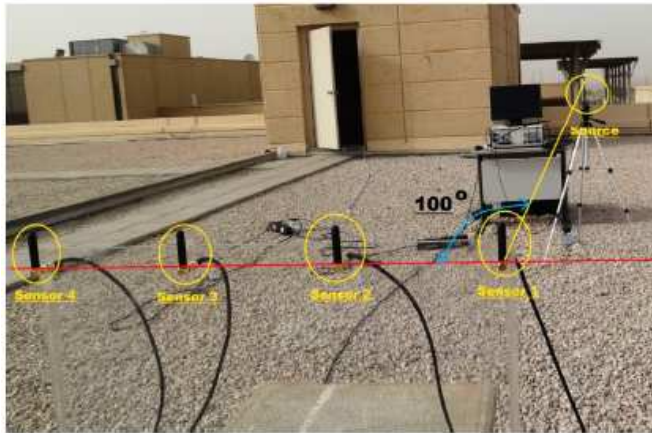


**Figure 10.** Experimental configuration for a single RF source placed at 100° from the array reference.
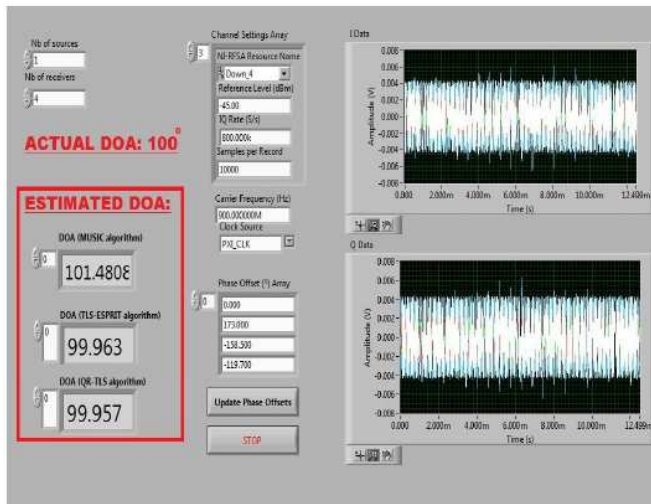


**Figure 11.** Experimental results for a single RF source placed at 100° from the array reference.

The experimental results of the proposed QR-TLS, MUSIC and ESPRIT algorithms for the first case of source angle are shown in Figure 11. The figure shows the estimated DOAs of 101.48°, 99.96°, and 99.95°, respectively. In order to confirm the experimental angles, the source angle is also measured manually with a protractor and a string extended from the source antenna to the reference antenna of the ULA. The manually measured source angle is 100° indicates close experimental estimates obtained with the proposed and the existing methods. The signal strengths of the received signals are shown in Figure 12 which shows an average signal power of around 35 dBm which lies within an acceptable range.
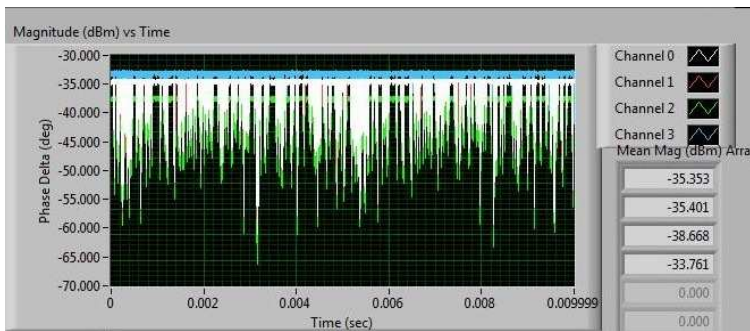


**Figure 12.** Received signal strength for a single RF source placed at 100° from the array reference.
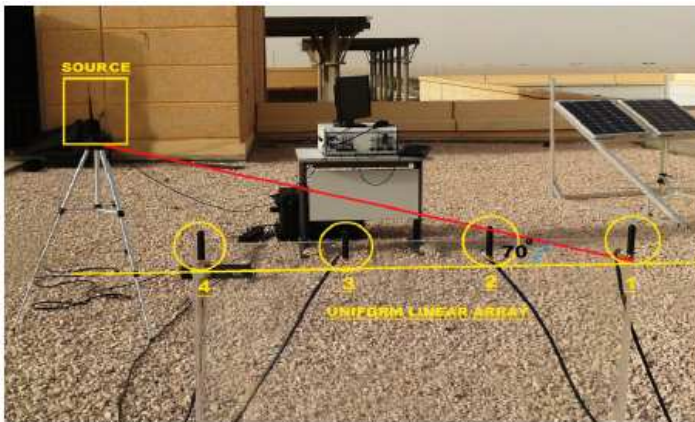


**Figure 13.** Experimental configuration, a single RF source placed at 70° from the array reference.

Another experimental configuration for the verification of the DOA estimation implementation method is shown in Figure 13. Similar to the first case, a single RF source is placed at an angle of 70° from the array reference in the far-field region of a ULA.

The DOA estimates obtained with the QR-TLS, MUSIC and ESPRIT methods are 67.33°, 71.37°, and 71.36°, respectively as shown in Figure 14. The source angle is also measured manually with a
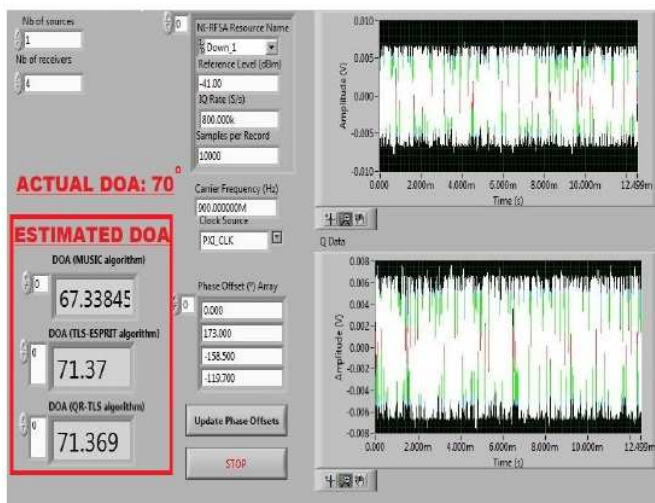


**Figure 14.** Experimental configuration, a single RF source placed at 70° from the array reference.
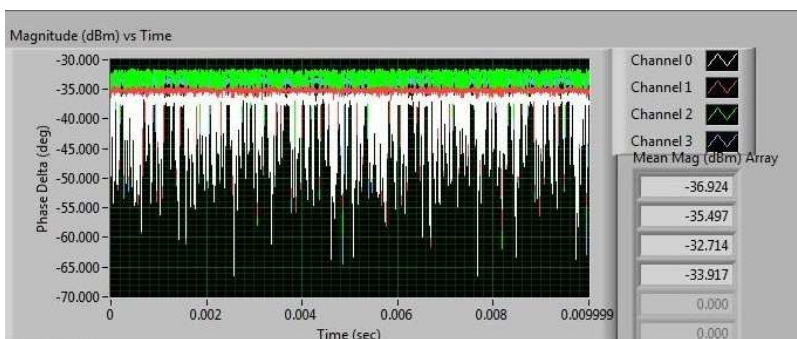


**Figure 15.** Received signal strength for a single RF source placed at 70° from the array reference.

protractor and a string which comes out to be 70° and hence indicating close experimental estimates. The signal strengths of the received signals are also shown in Figure 15 which shows an average signal power of around 38 dBm.

## 6.2. DOA Estimation for Two Sources

In order to assess the performance of the proposed method in real time for multiple incident sources, the experiments are also conducted for two cases of RF sources placed in the far-field region of a ULA. In the first case, the sources are placed at manually measured angles of 104° and 64° respectively from the array reference where the first antenna of the ULA is considered as an array reference. The experimental configuration for the first case is shown in Figure 16. The numbered circles in the figure show the ULA of antennas while the two boxes show two RF sources. The lines drawn from the reference antenna to the sources represent the two angles of arrival. The two DOA estimates obtained with the QR-TLS, MUSIC and ESPRIT methods are (65.54°, 104.41°), (64.38°, 104.65°), and (64.46°, 104.48°), respectively, as shown in Figure 17.

In the second case, the source positions are slightly altered and are placed at angles of 91° and 68° respectively from the array reference. Figure 18 shows the experimental configuration where numbered circles show the ULA of antennas while the two boxes show the two RF sources and the lines show the bearing angles of the two sources from
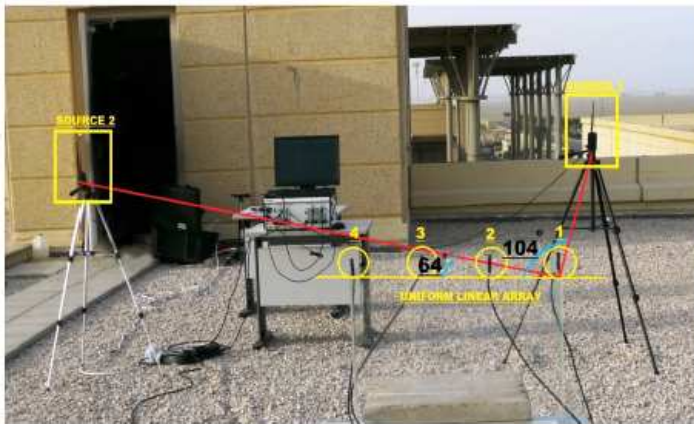


**Figure 16.** Experimental configuration, two RF sources placed at 64° and 104° from the array reference.

**Figure 17.** Experimental results for two RF sources placed at 65° and 104° from the array reference.
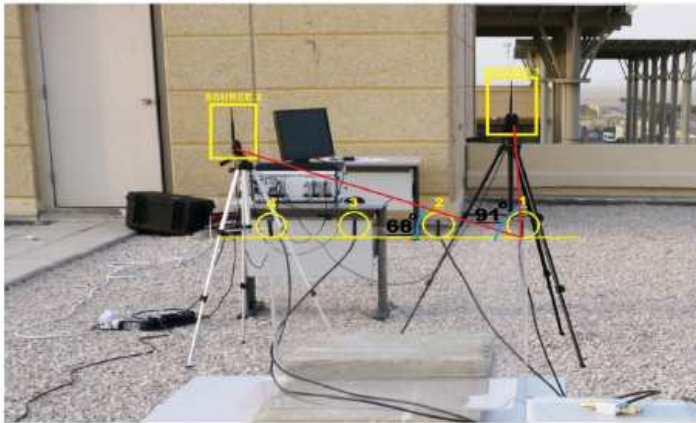


**Figure 18.** Experimental results for two RF sources placed at 68° and 91° from the array reference.

the reference antenna. The two DOA estimates obtained with the QR-TLS, MUSIC and ESPRIT methods are (69.95°, 91.96°), (69.31°, 90.65°), and (68.04°, 91.52°), respectively as shown in Figure 19. The proposed and the existing algorithms give close estimates of the DOAs to the actual measured angles.
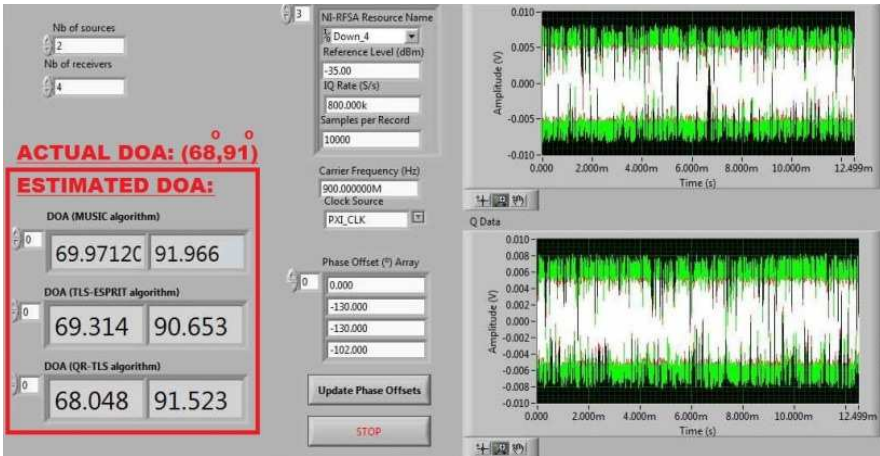
**Figure 19.** Experimental results for two RF sources placed at 68°
and 91° from the array reference.

## 7. CONCLUSIONS

An experimental verification of a proposed QR-TLS method of DOA
estimation is presented along with other two well known algorithms
MUSIC and ESPRIT for multiple incident source signals on a NI PXI
platform. The experimental implementation is outlined which includes
interfacing the ULA of antennas with a NI-PXI platform, phase
difference calibration at the receiver end, and transmitter and receiver
parameters selection for determining the DOAs of the multiple incident
source signals. The experimental results for test cases are presented for
both single and two RF sources lying at arbitrarily selected angles. The
results indicate successful real time implementation of the proposed
and the existing methods.

## REFERENCES

1. Zhang, Y., Z. Ye, X. Xu, and J. Cui, "Estimation of two-
   dimensional direction-of-arrival for uncorrelated and coherent
   signals with low complexity," *IET Radar, Sonar & Navigation*,
   Vol. 4, No. 4, 507–509, 2010.
2. Paulraj, A., R. Roy, and T. Kailath, "Estimation of signal
   parameters via rotational invariance techniques — ESPRIT,"
   *Nineteenth Asilomar Conference on Circuits, Systems and
   Computers*, 83–89, 1985.

3. Yang, P., F. Yang, and Z.-P. Nie, "DOA estimation with sub-array divided technique and interpolated ESPRIT algorithm on a cylindrical conformal array antenna," *Progress In Electromagnetics Research*, Vol. 103, 201–216, 2010.

4. Kim, Y.-S. and Y.-S. Kim, "Improved resolution capability via virtual expansion of array," *Electronics Letters*, Vol. 35, No. 19, 1596–1597, 1999.

5. Park, G.-M. and S.-Y. Hong, "Resolution enhancement of coherence sources impinge on a uniform circular array with array expansion," *Journal of Electromagnetic Waves and Applications*, Vol. 21, No. 15, 2205–2214, 2007.

6. Ichige, K. and H. Arai, "Implementation of FPGA based fast DOA estimator using unitary MUSIC algorithm [cellular wireless base station applications]," *IEEE 58th Vehicular Technology Conference, VTC2003-Fall*, Vol. 1, 213–217 2003.

7. Ichige, K. and H. Arai, "Real-time smart antenna system incorporating FPGA-based fast DOA estimator," *IEEE 60th Vehicular Technology Conference, VTC2004-Fall*, Vol. 1, 160–164, 2004.

8. Wang, H. and M. Glesner, "Hardware implementation of smart antenna systems," *Adv. Radio Sci.*, Vol. 4, 185–188, 2006.

9. Chen, J., J. Benesty, and Y. A. Huang, "Performance of GCC- and AMDF-based time-delay estimation in practical reverberant environments," *EURASIP Journal on Advances in Signal Processing*, Vol. 2005, No. 1, 25–36, 2005.

10. Hua, M.-C., C.-H. Hsu, and H.-C. Liu, "Implementation of direction-of-arrival estimator on software defined radio platform," *2012 8th International Symposium on Communication Systems, Networks & Digital Signal Processing (CSNDSP)*, 1–4, 2012.

11. Hou, S., S. Chang, H. Hung, and J. Chen, "DSP-based implementation of a real-time DOA estimator for underwater acoustic sources," *Journal of Marine Science and Technology*, Vol. 17, No. 4, 320–325, 2009.

12. Tayem, N., M. Omer, S. Raza, and M. Lakkis, "QR-TLS ESPRIT for source localization and frequency estimations," *Asilomar Conference on Signals and Systems*, 1–5, 2013.

13. Trefethen, L. N. and D. Bau, "Numerical linear algebra," *Society for Industrial and Applied Mathematics (SIAM)*, 1997.

14. Schmidt, R., "Multiple emitter location and signal parameter estimation," *IEEE Transactions on Antennas and Propagation*, Vol. 34, No. 3, 276–280, Mar. 1986.